RESEARCH ARTICLE

NANO · MICRO small
www.small-journal.com

The Stokes–Einstein–Sutherland Equation at the Nanoscale Revisited

Andreas Baer, Simon E. Wawra, Kristina Bielmeier, Maximilian J. Uttinger, David M. Smith, Wolfgang Peukert, Johannes Walter, and Ana-Sunčana Smith**

The Stokes–Einstein–Sutherland (SES) equation is at the foundation of statistical physics, relating a particle's diffusion coefficient and size with the fluid viscosity, temperature, and the boundary condition for the particle-solvent interface. It is assumed that it relies on the separation of scales between the particle and the solvent, hence it is expected to break down for diffusive transport on the molecular scale. This assumption is however challenged by a number of experimental studies showing a remarkably small, if any, violation, while simulations systematically report the opposite. To understand these discrepancies, analytical ultracentrifugation experiments are combined with molecular simulations, both performed at unprecedented accuracies, to study the transport of buckminsterfullerene C_{60} in toluene at infinite dilution. This system is demonstrated to clearly violate the conditions of slow momentum relaxation. Yet, through a linear response to a constant force, the SES equation can be recovered in the long time limit with no more than 4% uncertainty both in experiments and in simulations. This nonetheless requires partial slip on the particle interface, extracted consistently from all the data. These results, thus, resolve a long-standing discussion on the validity and limits of the SES equation at the molecular scale.

1. Introduction

Diffusion was first described by Robert Brown in 1827,[1] who observed jittering of small particles in water. The fundamental framework for this phenomenon, however, emerged only a century later due to contributions of Einstein,[2] Sutherland,[3] and Smoluchowski.[4] First, the Stokes–Einstein–Sutherland (SES) equation was developed relating the diffusion coefficient to temperature and the Stokes force acting on the moving particle. Second, Einstein and Smoluchowski provided the keystone for the fully probabilistic formulation of diffusion. The latter was experimentally confirmed by Jean–Baptiste Perrin and his students in 1908.[5–8]

While very simple, easy to use, and often applied for particle size determination,[9–13] the SES equation applies in the thermodynamic limit and requires a separation of scales between the particle and the solvent in terms of mass and size.[14–16] Therefore, it should break down for diffusive transport at the molecular scale. Surprisingly, however, experimental studies often confirm the appropriateness of the SES prediction for molecular diffusion, despite the clear limits imposed by the theoretical framework.[17]

The paradigmatic systems for studies of the SES equation have been the buckminsterfullerenes due to their stability and well-defined shape. Specifically, Soret forced Rayleigh scattering was used to measure the diffusion coefficient of C_{60}

A. Baer, S. E. Wawra, K. Bielmeier, M. J. Uttinger, W. Peukert, J. Walter
Department of Physics
PULS Group
Interdisciplinary Center for Nanostructured Films (IZNF)
Friedrich-Alexander-Universität Erlangen-Nürnberg
Cauerstr. 3, 91058 Erlangen, Germany
E-mail: johannes.walter@fau.de

S. E. Wawra, K. Bielmeier, M. J. Uttinger, W. Peukert, J. Walter
Institute of Particle Technology (LFG)
Friedrich-Alexander-Universität Erlangen-Nürnberg
Cauerstr. 4, 91058 Erlangen, Germany

D. M. Smith, A.-S. Smith
Interdisciplinary Center for Functional Particle Systems (FPS)
Friedrich-Alexander-Universität Erlangen-Nürnberg
Haberstr. 9a, 91058 Erlangen, Germany
E-mail: smith@physik.fau.de

A.-S. Smith
Division of Physical Chemistry
Group of Computational Life Sciences, Ruđer Bošković Institute
Bijenička 54, Zagreb 10000, Croatia

The ORCID identification number(s) for the author(s) of this article can be found under https://doi.org/10.1002/smll.202304670

DOI: 10.1002/smll.202304670

in *o*-dichlorobenzene.[18] They compared the radius of C_{60}, extracted using the SES equation, to partial molecular volume measurements.[19] With measurement errors of up to 10%, their measured deviation of the SES equation was less than 15%, using slip boundary conditions on the particle-solvent interface.

C_{60} as well as C_{70} was used again more recently to verify the performance of the SES equation in analytical ultracentrifugation (AUC) experiments.[20] Deviations of only about 5% were found, this time with stick boundary conditions. The reference size of fullerenes was taken from the size of the rigid carbon shell,[21–26] which notably ignore solvation effects. Furthermore, in these experiments, neither finite concentration effects of C_{60} and C_{70} have been taken into account nor has the statistical significance of the results been checked. Finally, the choice of the boundary conditions was restricted to stick or slip with the conclusion that stick boundary conditions provide better results.

An alternative approach to study the limits of the SES equation is molecular dynamics (MD) simulations. They are the ideal tool for this task because they explicitly account for the atomic nature of the interactions, as well as for all the relevant time and length scales. However, unlike experiments, MD simulations systematically demonstrate discrepancies from the SES equation for small particles.[16,27–35] However, the accuracy of the results was often questioned due to finite system sizes[27,29–31] and limited sampling[30,32,35] of slowly convergent power law decays.[36] Interestingly, systematic simulation studies of fullerenes have not yet been performed. In order to understand the apparently small deviations of the SES equation in experiments, and large deviations in simulations, we here perform AUC measurements as well as MD simulations of C_{60} suspended in toluene. Our aim is to combat issues of accuracy and sampling to explore the implication of different physical assumptions in modeling and measuring diffusion on the molecular scale as well as the influence of the partial molecular volume. This joint experimental and theoretical effort allows us to address the applicability of the SES equation in the infinite dilution limit, and use the precise analysis to determine the appropriate boundary conditions at the fullerene-solvent interface. We are, therefore, able to explore advantages and limitations of each approximation used to define the SES equation and hence provide a clear explanation of systematic discrepancy between experimental and modeling efforts appearing over several decades.

2. Stokes–Einstein–Sutherland Equation and Equilibrium Statistical Mechanics

2.1. Theoretical Consideration

In 1905, both Einstein[2] and Sutherland[3] published the well-known relation between the diffusion and friction coefficients D and ξ, respectively, of a particle in a solvent

$$D = \frac{k_B T}{\xi} \tag{1}$$

Here, T is the temperature and k_B the Boltzmann constant. Both Einstein and Sutherland used the Stokes' formula to express the friction coefficient as a function of the fluid shear viscosity η and the hydrodynamic radius R_H of the particle, which was assumed to be spherical:

$$\xi = b\pi\eta R_H \tag{2}$$

The prefactor b is a function of the boundary condition on the particle-solvent interface and ranges from 4 for a perfect slip to 6 for a perfect stick boundary condition, as used by Stokes[37] and Einstein.[2] Finally, by combining Equations (1) and (2) one obtains the SES equation

$$D = \frac{k_B T}{b\pi\eta R_H} \tag{3}$$

for the diffusion coefficient of a particle dispersed in a liquid.

This approach surprisingly well relates molecular fluctuations, characterized by diffusion, with a highly coarse grained hydrodynamic friction, where molecular details are no longer resolved. Instead, they are incorporated into the boundary condition b. The friction itself is defined as the ratio of a force F acting on the particle and the velocity v resulting from this force

$$\xi = \frac{F}{v} \tag{4}$$

Already in the original derivation,[2,3] the force acting on the particle was presumed to arise from its collisions with the solvent molecules that in equilibrium should average to zero in the long time limit.

Significant progress in understanding the relation of transport coefficients to microscopic degrees of freedom as well as the limits of applicability of the SES equation in terms of involved time and length scales was achieved using techniques from statistical mechanics.[14,38–44] Building on the molecular theory, it became possible to express transport coefficients as integrals of autocorrelation functions of a corresponding dynamic variable using the so called Green–Kubo (GK) relations.[38–40,42] For example, the shear viscosity could be calculated from the off-diagonal elements of the stress tensor $P_{\alpha\beta}$

$$\eta = \frac{V}{k_B T}\int_0^\infty \langle P_{\alpha\beta}(t)P_{\alpha\beta}(0)\rangle \mathrm{d}t \tag{5}$$

where the brackets $\langle . \rangle$ denote an ensemble average. Most notably, the diffusion coefficient was found to be related to the velocity autocorrelation function (VACF) with

$$D_{\mathrm{VACF}} = \int_0^\infty \langle v(t)v(0)\rangle \mathrm{d}t \tag{6}$$

while the friction coefficient was related to the stochastic force $F_S(t)$ acting on the particle of interest through its autocorrelation function[38,43–45]

$$\xi = \frac{1}{k_B T}\int_0^\infty \langle F_S(0)F_S(t)\rangle \mathrm{d}t \tag{7}$$

The latter equation can be obtained from a general Langevin equation

$$\frac{\partial}{\partial t}p(t) = -\int_0^t \mathrm{d}sK(s)p(t-s) + F_\mathrm{S}(t) \tag{8}$$

where $p(t)$ is the particle momentum, $K(s)$ the memory kernel, and $F_\mathrm{S}(t)$ a stochastic force acting on the particle. The fluctuation-dissipation theorem relates the memory kernel to the stochastic force via

$$\langle F_\mathrm{S}(t)F_\mathrm{S}(t')\rangle = 3k_\mathrm{B}TK(t-t') \tag{9}$$

and the integral of the memory kernel yields Equation (7). Obtaining the stochastic force autocorrelation function (F_SACF), required for the memory kernel, from simulations or experiments is a non-trivial task.[46] However, upon deriving this formula via the projection operator formalism[44,45] (cf. Section SI A, Supporting Information, for the derivation), and assuming a small rate of change of the particle momentum, that is,

$$\frac{\partial}{\partial t}p(t) = \mathcal{O}(\lambda) \tag{10}$$

with some small parameter λ, the F_SACF can be approximated with the total force autocorrelation function (F_TACF)

$$\langle F_\mathrm{S}(t)F_\mathrm{S}(t')\rangle = \langle F_\mathrm{T}(t)F_\mathrm{T}(t')\rangle + \mathcal{O}\left(\lambda^3\right) \tag{11}$$

upon neglecting orders of λ^3 and higher. The total force F_T is easily accessible through Newton's equation $F_\mathrm{T} = \partial p/\partial t$, especially from MD simulations, where it is a prognostic variable. The friction coefficient is then given as

$$\xi = \frac{1}{k_\mathrm{B}T}\int_0^\infty \langle F_\mathrm{T}(0)F_\mathrm{T}(t)\rangle \mathrm{d}t \tag{12}$$

Notably, it was shown, that the zero frequency component of the F_TACF and hence its time integral, will be non-zero if and only if the limit $\lambda \to 0$ is strictly fulfilled,[15,38,43,47,48] which corresponds to a particle with constant momentum, often referred to as the frozen particle. Nonetheless, invoking Stokes' formula in Equation (2) for a particle with constant, non-zero momentum also fulfills this limit. Furthermore, both the autocorrelation functions of velocity (Equation (6)) and position (not shown here) do have a zero frequency component and can thus be used to obtain the friction coefficient,[48] which is equivalent to invoking the Einstein–Sutherland equation. The statistical approach therefore provides Equation (1) from first principles and sets the limits of applicability of the SES equation.

2.2. Molecular Dynamics Simulations

To assess how crucial the restriction of the constant particle momentum is, we reformulate the problem (cf. Section SI A, Supporting Information, for the derivation), to obtain a Volterra equation of first kind, that can be directly checked from simulations:

$$\frac{\partial}{\partial t}\langle p(t)p(0)\rangle = -\frac{1}{k_\mathrm{B}T}\int_0^t \mathrm{d}s\langle F_\mathrm{T}(s)F_\mathrm{T}(0)\rangle \cdot \langle p(t)p(0)\rangle \tag{13}$$

This equation includes approximating the F_SACF with the F_TACF.

MD simulations are performed using the GROMACS simulation package,[49–55] by placing a single C_{60} in a box of toluene (cf. **Figure 1**a) and applying periodic boundary conditions (see Section SII A, Supporting Information, for details). For toluene, we use the Optimized Potentials for Liquid Simulations (all atoms) (OPLS-AA) force field,[56] while the parameters for C_{60} are taken from previous work.[57] Following an extensive protocol to equilibrate the system at room temperature and 1 bar, production simulations are performed in NVT ensemble with the temperature maintained by the Nosé–Hoover thermostat. We modify the output routine of GROMACS to simultaneously extract the total force on the particle and its momentum with the output rate of 10 fs without all solvent information. This accounts for C_{60} internal forces and external van der Waals forces, while Coulomb forces are absent for the uncharged C_{60} atoms. To take into account finite size effects we simulate an array of systems with 478 to 46838 toluene molecules (Figure 1a), for in total 0.6 to 35 µs, and apply the appropriate finite size corrections.[58,59] Using the system isotropy, averaging over all spatial dimensions is performed to improve the statistics.

This methodology allows us to evaluate both sides of Equation (13) by numerical differentiation or integration. We find that this expression does not hold for a C_{60} in toluene, which clearly demonstrates that the momentum is not a slowly changing variable (Figure 1b). Thus, one could infer that the friction coefficient cannot be properly obtained by the Green–Kubo approach, which becomes evident from directly evaluating Equation (12). The full integral vanishes as expected.[38,48] Other methods were previously suggested to calculate the friction coefficient from the running integral of the F_TACF,[15,16,32] which worked for particles heavy compared to the solvent molecules but not necessarily infinitely heavy. In our case, neither a linear nor an exponential decay can be observed (cf. Section SIII A4 and Figure S8, Supporting Information) and thus the only method left is using the maximum of the running integral, that corresponds to the first zero-crossing of the F_TACF, as suggested by Lagar'kov and Sergeev.[60] This method, known to be an overestimation,[15,32] yields with corrections for finite size effects (see Section SIII A1 and Equation (S28), Supporting Information) $\xi = (3.37 \pm 0.03) \times 10^{-12}\,\mathrm{kg\,s^{-1}}$.

This can be verified by extracting the diffusion coefficient of C_{60} from the VACF via the Green–Kubo relation (Equation (6)) and the mean square displacement (MSD) (cf. Section SIII A3, Supporting Information) as both methods are well established[16,36] (cf. **Figure 2**a,b). We account for the finite size effects by the theoretical size dependence of the diffusion coefficient,[58,59] adjusted to include a variable boundary condition b

$$D_\infty = D_\mathrm{PBC} + \frac{k_\mathrm{B}T\zeta}{b\pi\eta a} \tag{14}$$

Using this equation, all data (cf. Figure 2c) can be fitted (blue circles and orange squares) or corrected (green diamonds and red triangles). Hereby, the fit was calculated by treating both the boundary condition parameter b and the infinite diffusivity D_∞ as free parameters, yielding $D_\infty = (5.67 \pm 0.19) \times 10^{-10}\,\mathrm{m^2\,s^{-1}}$ for

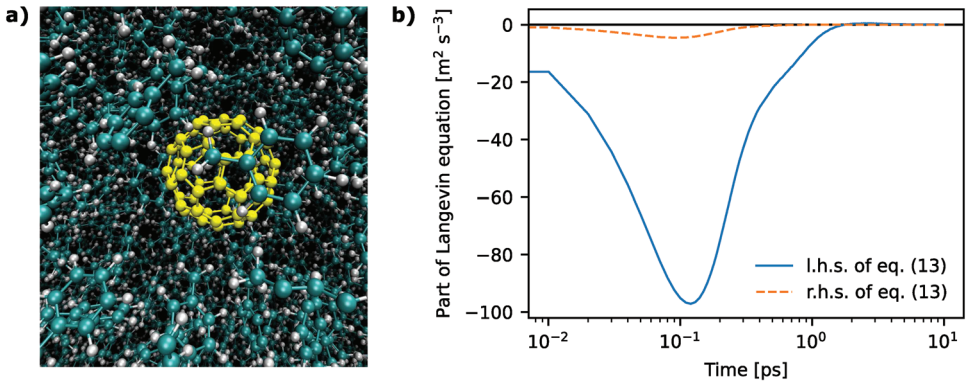

Figure 1. C_{60} in toluene as a model for studying molecular diffusion. a) The system in question: A single C_{60} (colored in yellow) is dispersed in toluene. b) Comparison between left and right hand side of Equation (13). The left hand side is nearly 20 times larger than the right hand side. In addition, the sign is different in the regime from 1.0 to 1.7 ps, demonstrating that the momentum of C_{60} cannot be treated as a slow variable. Ensemble averages cover 3D trajectories of the same system size with 3824 solvent molecules and a total simulation time of ≈35 µs.

the VACF and $D_\infty = (5.65 \pm 0.17) \times 10^{-10}\,\mathrm{m^2\,s^{-1}}$ for the MSD. Unfortunately, the parameter b carries a significant uncertainty, such that precise conclusions about the effective boundary condition cannot be made using this approach.

Using Equation (1), we compare the obtained D_∞, with the calculated $k_B T/\xi$. We find deviations larger than 50%, due to the gross underestimation of the C_{60} friction coefficient. This clearly shows that the standard approximations of equilibrium statistical physics underlying the SES equation do not hold in this system, presumably because of the similar mass of the C_{60} and the toluene molecule.

As this deviation stems from the failure of approximating the memory kernel $K(s)$ with the F_TACF instead of the F_SACF, it is only natural to verify whether the memory kernel, if extracted with different methods,[46] reproduces the correct friction coefficient. Several methods to derive the memory kernel for systems on the molecular scale have been developed in the past years.[46] We calculate $K(s)$ through the Fourier transform from the VACF, as suggested by refs. [46, 61] which is equivalent to calculating the diffusion coefficient from the VACF and invoking the Einstein–Sutherland equation (Equation (1)). For the system with 3824 solvent molecules, we obtain a clear deviation from the kernel obtained from the F_TACF (see Figure S9a, Supporting Information). By integrating the kernel from the VACF, we obtain $\xi_{PBC} = (8.68 \pm 0.03) \times 10^{-12}\,\mathrm{kg\,s^{-1}}$, which, by the Einstein–Sutherland equation (Equation (1)), corresponds to a diffusion coefficient of $D_{PBC} = (4.66 \pm 0.02) \times 10^{-10}\,\mathrm{m^2\,s^{-1}}$, precisely the value obtained by integrating the VACF (both values are for the same system size and thus not corrected for system size effects). This expected agreement underlines the failure of approximating the F_SACF with the F_TACF for such small particles, while supporting the validity of the Einstein–Sutherland equation.

3. Einstein–Sutherland Equation under Conditions of Constant Drag

3.1. Analytical Ultracentrifugation Experiments

There are several reports that validate the SES equation for C_{60} in molecular solvents.[17,18,20] However, even these works differ in the choice of the boundary conditions and treatment of effects of finite concentration. This, together with the results of the previous section, calls for a discussion of the validity of the theory and/or the correct choice of parameters for comparison.

To clarify these issues, we perform a set of AUC experiments to observe the reaction of the system to a centrifugal field.[62–64] In this type of experiments, referred to as sedimentation velocity AUC (SV-AUC) experiments, we resolve the temporal evolution and radial distribution of the particles' concentration (cf. Section SII B, Supporting Information). Using numerical solutions of the Lamm equation (Equation (S14), Supporting Information), we fit the data with the diffusion and sedimentation coefficients D and s, respectively, while also considering compressibility of the solvent (cf. Sections SI B, SII C and SIII A7, Supporting Information, for details). Conducting the experiment at different concentrations (**Figure 3**), allows us to retrieve the values extrapolated to infinite dilution by means of a linear fit to be $D_0 = (7.41 \pm 0.04) \times 10^{-10}\,\mathrm{m^2\,s^{-1}}$ and $s_0 = (1.26 \pm 0.01)$ sved. The single sample measurement of Pearson et al.[20] at a finite concentration, which we estimate to be about 1 g L^{-1}, yields $D_{Pearson} = (7.59) \times 10^{-10}\,\mathrm{m^2\,s^{-1}}$, which is fully consistent with our data.

However, direct comparison of the measured diffusion coefficients to simulation results (Section 2.2) shows significant differences. This discrepancy can be attributed to the 1.4 times higher viscosity of toluene provided by the OPLS-AA force field[56] (see Section SIII A2, Supporting Information) compared to experimental reference measurements at same thermodynamic conditions of a temperature of 293.15 K and pressure of 1 bar.[65] We can, nonetheless, normalize the diffusion coefficient by the ratio of the MD and measured viscosity (Section SIII A2, Supporting Information), which provides an agreement between the simulated and the experimental diffusivity with a deviation of less than 10% (see Table 2, column 4).

We can then obtain the friction coefficient directly from $s_0 = m/\xi$, with m being the excess mass of the analyte, that is, the mass of the analyte minus the mass of solvent with the same volume. Ruelle et al.[19] measured the C_{60} partial molecular volume in toluene to be 0.603 nm^3, which combined with its molecular mass of 720.66 u and a toluene density of 866.86 $kg\,m^{-3}$

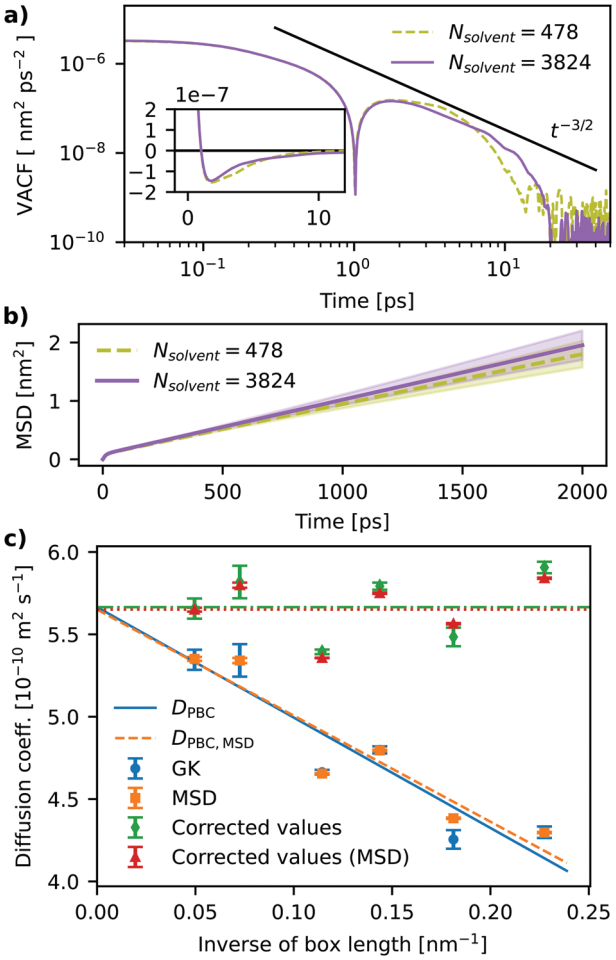

Figure 2. Diffusion coefficient of C_{60} in toluene obtained from MD simulations. a) Log–log representation of the absolute value of the VACF for two different system sizes (inverse of box length: ≈0.23 and 0.11 nm^{-1}). The analysis runs over 6 and 35 µs 3D trajectory, for the small and large systems, respectively. Especially for the larger system, the expected decay proportional to $t^{-3/2}$ is apparent for times >2 ps.[36] The inset shows a lin–lin representation of the VACF in the region around the first minimum. b) MSD for the same system sizes as in (a). Due to finite size effects, the larger system produces a larger MSD and diffusion coefficient (cf. panel (c)). c) Size dependence of the diffusion coefficient. Equation (14) is used for both the fit (lines) and the corrected values. Symbols represent mean and standard deviation of the plateau region for a single system size each (cf. Figure S1, Supporting Information). The analysis runs over 6 to 35 µs 3D trajectory, for the different systems.

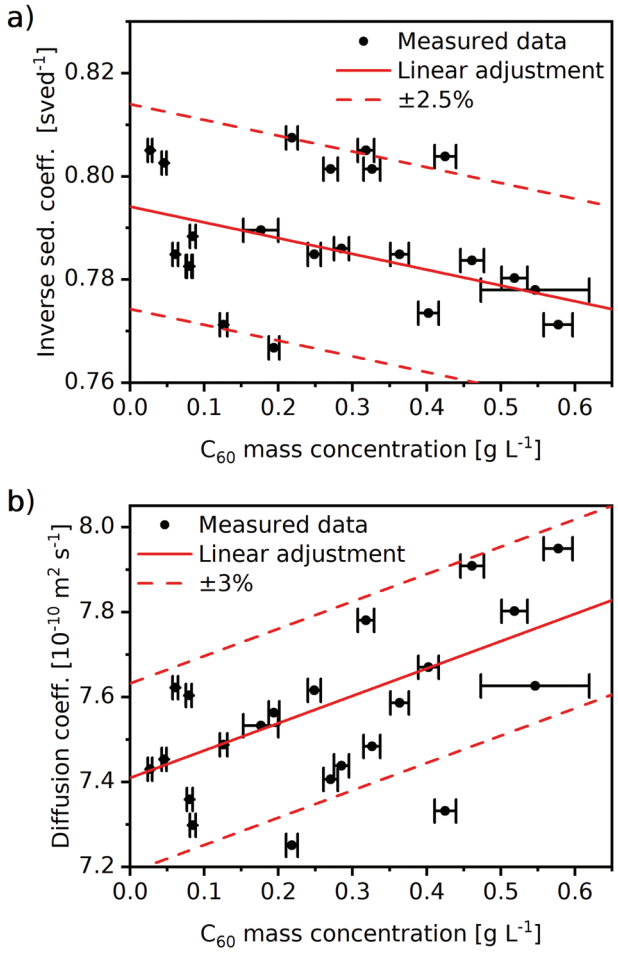

Figure 3. a) Retrieved inverse sedimentation coefficients and b) diffusion coefficients from SV-AUC experiments as a function of C_{60} mass concentration. Depicted are hydro- and thermodynamic non-ideality of C_{60} resulting from data-analysis with the $c(s)$-model (Levenberg–Marquardt). Linear fits were performed taking the uncertainty of the extinction, optical path length, and the extinction coefficient at 570 nm for the concentrations into account. The corresponding uncertainty (standard deviation) is depicted with the symbols.

yields a friction coefficient of $5.35\times 10^{-12}\,kg\,s^{-1}$. We can now compare this to the prediction of the Einstein–Sutherland equation (Equation (1)) obtained from the diffusion coefficient of the AUC experiments, which gives $k_B T/D_0 = 5.46 \times 10^{-12}\,kg\,s^{-1}$. Both results agree within 2%,clearly demonstrating the validity of the Einstein–Sutherland equation for this system, which was not explicitly shown before. We hypothesize that this estimate of friction stems from the non-equilibrium nature of the AUC experiment. Namely rather than the friction being measured as a response to the stochastic force, here it emerges from the response to a constant drag or centrifugal force acting on the C_{60}.

3.2. Friction as Response to a Drag Force in Non-Equilibrium MD Simulations

To verify our hypothesis that the friction coefficient can be determined if a particle is subject to a non-vanishing average force, we return to modeling and perform non-equilibrium molecular dynamics NEMD simulations. Specifically, an additional (constant) force on the fullerene is added while removing the center-of-mass motion of the entire system. The latter is required to obtain a proper frame of reference with periodic boundary conditions. The resulting particle velocity, relative to the fluid, is then calculated and combined with the known force to extract the friction coefficient ξ from Equation (4).

To ensure, that we sample the linear regime, a set of pull forces is investigated (cf. **Figure 4** and Section SIII A6, Supporting Information). For weak pull forces (blue points in Figure 4), the sampling is poor due to the small signal-to-noise ratio, while

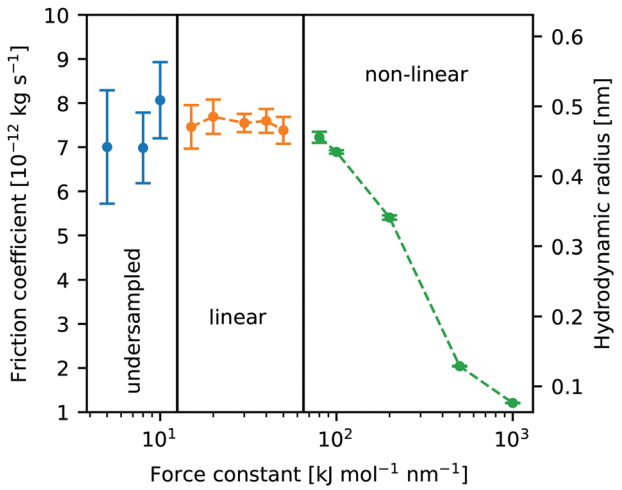

Figure 4. Friction coefficient of C_{60} obtained from steered MD simulations. The friction coefficient ξ_{PBC} is calculated for each applied constant force as the ratio of applied force and resulting average velocity. Three regimes are indicated, the regime where statistics are not sufficient to determine a precise friction coefficient, the regime of proper linear response and the regime of non-linear response, where the apparent friction coefficient drops significantly. For the present study, only the linear regime is relevant and used to determine the friction coefficient as the mean over the entire range. Displayed error bars denote the uncertainty in the mean of the calculated friction coefficient, where the mean is calculated over a total of 40–200 ns trajectory. The hydrodynamic radius displayed corresponds to a boundary condition value of $c = 6$.

for large pull forces (green points), non-linear effects arise. For intermediate pull forces (orange points), we observe a properly converged and linear regime. Accounting for finite size effects (Equation (S28)) yields $\xi = (6.9 \pm 0.15) \times 10^{-12}\,\mathrm{kg^2\,s^{-1}}$ Notably, this again compares well (about 10% deviation) to the AUC result, when corrected for the differences in the viscosity (cf. Section 3.1).

Importantly, we can calculate the diffusion coefficient from this friction coefficient with the Einstein–Sutherland equation (Equation (1)) to obtain $D = (5.9 \pm 0.1) \times 10^{-10}\,\mathrm{m^2\,s^{-1}}$, with the statistical error of 2%. This is basically the same result as the diffusion coefficient obtained from the MSD or the VACF (Section 2.2). This confirms the validity of the Einstein–Sutherland equation found in the AUC experiments also for MD simulations, rendering both techniques consistent.

4. Stokes–Einstein–Sutherland Equation

4.1. The Effective Radius of C_{60}

With the validity of the Einstein–Sutherland equation demonstrated for both experiments and NEMD simulations, the next step is to assess the validity of the SES equation and more importantly to retrieve a proper value for the boundary condition coefficient b. To assess this, we need to calculate and/or measure toluene viscosity (Section SIII A2, Supporting Information), and the hydrodynamic radius of the C_{60} independently from the friction and diffusion coefficients.

As the C_{60} is a very rigid, nearly spherical molecule that does not feature extraordinarily strong interactions with the carbon-rich toluene, solvation effects in this specific environment were found to be very small compared to the C_{60} in the solid phase.[19] This is reflected in sub-angstrom differences in radii R_V, that can be associated to a sphere with equivalent volume (cf. refs. [19, 22–25, 66–70], **Table 1**, and Section SIII C, Supporting Information). Because of these small differences, R_V has been used as the estimate for the C_{60} hydrodynamic radius R_H.[20]

To verify these results and validate our own simulation and experimental protocols, we pursue the independent calculation of the partial molecular volume. In simulations, the partial molecular volume can be obtained from the particle-solvent radial distribution function $g(r)$ via a Kirkwood–Buff integral[71]

$$V = \frac{4}{3}\pi R_V^3 = \frac{1}{n_s} + 4\pi \int_0^\infty [g_s(r) - g(r)] r^2 \mathrm{d}r \tag{15}$$

with $g_s(r)$ being the radial distribution function of the pure solvent and n_s the number density of the solvent (cf. Figure S11a, Supporting Information). This provides $R_V^{sim} = 0.500 \pm 0.003\,\mathrm{nm}$, deviating from the experimental ref. [19] by only 4%.

We, furthermore, independently determine the C_{60} radius in experiments, using sedimentation equilibrium AUC experiments with density contrast. In these measurements, the rotor speed and thus centrifugal force is sufficiently small such that the sedimentation flux compensates the diffusion flux at each radial position. From the resulting exponential concentration profile, the apparent buoyant mass can be calculated independent of the viscosity. Using solvents with different levels of deuteration, which changes solvent density but not the solvation properties of dissolved species, the partial specific volume (PSV) can be obtained. Due to a small number of parameters and thus small statistical uncertainties, the relevant data can be obtained with high accuracy yielding $R_V^{exp,DC} = 0.526 \pm 0.014\,\mathrm{nm}$, which is within measurement errors of less than 3% compared to literature results obtained using different methods,[19] and only 5% different to the simulation data. Finally to check the consistency of our SV-AUC experiments, we retrieve the PSV directly from the diffusion and sedimentation coefficients at the infinite dilution limit by rearranging the well-known Svedberg

Table 1. Summary of radii of the C_{60} obtained by various methods. The radius $R_{graphite}^{exp}$ is obtained by adding half of the graphite interplanar distance to the radius of the structure of the C_{60} nuclei, which gives the radius in the gas phase. The radius R_{cryst}^{exp} is obtained by the fullerene distance in C_{60} crystal. All radii R_V are volume equivalent radii, that is, radii corresponding to the partial molecular volume or the partial specific volume.

Method	Source	Radius [nm]
$R_{graphite}^{exp}$	Refs. [22–24, 66–68]	0.522 ± 0.001[a)]
R_{cryst}^{exp}	Refs. [25, 69, 70]	0.52 ± 0.01[a)]
R_V^{sim}	Section 4.1	0.500 ± 0.003
$R_V^{exp,AUC}$	Section 4.1	0.520 ± 0.002
$R_V^{exp,DCSE}$	Section SIII C, Supporting Information	0.526 ± 0.014
R_V^{exp}	[19]	0.524 ± 0.003

[a)] This value is the average over several measurements reported in the literature (see Section SIII C, Supporting Information).

equation (Equation (S15), Supporting Information) to solve for the PSV (Equation (S32), Supporting Information). This gives $R_V^{exp,AUC} = 0.520 \pm 0.002$ nm. Notably, this is within measurement errors of less than 1% equivalent to the values obtained with our other approaches and the literature[19] (cf. Table 1).

4.2. Effective Boundary Condition at the C_{60} Toluene Interface

With these referent values for the C_{60} size, we can now proceed with the determination of the boundary condition at the particle-solvent interface. For the AUC experiments, the boundary condition value can be retrieved directly from the well-known frictional ratio ξ/ξ_0, which is also known as f/f_0 in the AUC literature. It is defined as the ratio of the friction coefficient of the analyte to the friction coefficient of a sphere of equal volume as the analyte and assuming stick boundary conditions. When expressed in terms of s and D and using the PSV $\bar{\nu}$ of the fullerene, one obtains for spherical particles the well-known form

$$\xi/\xi_0 = \left(\frac{\sqrt{2}}{18\pi} \frac{k_B T}{D\sqrt{s\eta^3}} \sqrt{\frac{1-\bar{\nu}\rho}{\bar{\nu}}} \right)^{\frac{2}{3}} = 0.95 \pm 0.01 \quad (16)$$

The frictional ratio is typically used to evaluate shape anisotropy and volume expansion due to solvation, when $\xi/\xi_0 \geqslant 1$.[63] With the nearly perfect spherical shape of C_{60} and hardly any volume expansion effects (see Sections SIII B and SIII C, Supporting Information), we expect a value very close to unity. However, values $\xi/\xi_0 < 1$, on the other hand, point to deviations from the stick boundary condition. Indeed, when assuming $R_H = R_V$, we obtain $b = 6 \cdot \xi/\xi_0 = 5.71 \pm 0.06$.

We can furthermore determine the boundary condition b at the C_{60}–toluene interface, such that the SES equation holds, also from simulations. Using D_{VACF} or D_{MSD} and Equation (3), with $R_H = R_V$ determined in simulations, we obtain $b = 5.3 \pm 0.2$. Following a similar strategy, we can combine experimental data in the literature (R_V^{exp}[19] and D_{AUC}[20]), and obtain $b = 5.54 \pm 0.03$, which is within the error bar of the simulation and only 3% smaller than our experimental results.

Due to significant accuracy of the measurements and simulations, these results clearly indicate that perfect stick boundary conditions, typically assumed in experiments[17,20,72–76] and simulations,[27,28,33–35] may not be the correct choice for C_{60}. Actually, with $b = 6$ systematic errors of 5% to 12% are found in simulations and experiments. Furthermore, R_H calculated from the SES is found to be *smaller* than R_V.

Finding deviations from the stick boundary conditions should not be surprising in the light of a long going discussion on its application for small particles.[77] The argument is captured by the Knudsen number Kn, the latter being defined as the ratio of mean free path and size of a particle. It can be calculated as $Kn = (\sqrt{2}\pi n d^2 l)^{-1}$, where n and d are number density and diameter of the solvent, while l is the characteristic length of the system. With d taken to be the diameter of the toluene aromatic ring and l the diameter of the fullerene, we estimate $Kn \approx 0.09$. This is significant because the Knudsen number can be used as a measure to determine b.[72] Specifically for $Kn = 0$, one expects perfect stick ($b = 6$) while for $Kn \to \infty$, perfect slip ($b = 4$). As soon as Kn is not vanishing, as in the present case, $b < 6$ should be obtained, which is indeed the case.

5. Discussion and Conclusions

We here present a set of experimental and simulation results on the dynamic and static properties of a C_{60} dispersed in toluene. We perform AUC experiments reporting diffusion and sedimentation coefficients in the infinite dilution limit, improving the accuracy of the method.[20] Instead of following the usual approach to AUC data and calculating the particle mass and size, we use the known mass of C_{60} to report the hydrodynamic radius and the boundary condition at the particle-solvent interface. We also perform a quantitative comparison of simulations and experiments, which is excellent for static properties derived from density distributions. This includes the determination of the partial molecular volume of C_{60}, which differs from the experimental estimate by only a couple of percent. Extracting dynamic properties such as viscosity is more challenging due to the limitations of current force fields. However, upon simple re-scaling by the viscosity contrast (column 4 in **Table 2**) the difference between observed and measured diffusivities is only 10%. Furthermore, the analysis, which does not rely on correcting for the viscosity contrast, allows us to make several important findings:

- The expression associating the F_TACF and the friction coefficient suggested by Kirkwood,[38] the Green–Kubo theory,[39–42] and the Mori–Zwanzig formalism[14,43,44] is the main starting point for the critique on the applicability of the SES equation at the nanoscale. In its derivation, the assumption that the particle momentum is constant, or only very slowly changing, is mandatory. We show that this assumption is clearly violated for C_{60} in toluene due to its small molecular weight ,[15,47] back-scattering, and dissipation of momentum through internal degrees of freedom that couple with directional motions on sub-picosecond time scales (Figure 1b). The F_TACF integrates these effects, resulting in a vanishing response of the zero frequency component, and thus, in this formulation, cannot be directly related to friction. If, contrastingly, the memory kernel is obtained from the F_SACF or via a different method,[46,61] the actual friction coefficient can be obtained.
- Another reliable measurement of the friction coefficient, however, can be obtained in non-equilibrium conditions. A good estimate can be extracted from the average velocity of C_{60} induced by a drag force in the linear response. This is permitted by the momentum conservation and the nanosecond sampling times when conditions of slow dynamics are recovered (Figure 1b). In experiments, the non-equilibrium conditions are provided in the sedimentation experiments, while in simulations, the friction is obtained in steered molecular dynamics (following Equation (4)). Using the Einstein–Sutherland relation, we can compare this friction to independently measured diffusion constants. For experiments, where infinite dilution sedimentation and diffusion coefficients are extracted by a sequence of measurements, the Einstein–Sutherland equation is recovered with 1% accuracy. In simulations, by accounting for finite size effects, the Einstein–Sutherland relation holds with a precision of <2%. This confirms the validity of the

Table 2. Summary of diffusion coefficients and boundary conditions of the C_{60} obtained by various methods. Values derived using Equation (1) are indicated by superscripts. All values except for the one obtained from the F_TACF match. We find the averaged value of $\bar{b} = 5.5 \pm 0.2$ (cf. Section 4.2) to be consistent with all other presented data.

Method	Source	Diffusivity [10^{-10} m^2 s^{-1}]	Rescaled diffusivity [10^{-10} m^2 s^{-1}]	b from SES [–]
F_TACF	Section SIII A4, Supporting Information	$12.0 \pm 0.1^{a)}$	$17.4 \pm 0.2^{a)}$	2.53 ± 0.04
VACF, MSD	Section 2.2	5.7 ± 0.2	8.2 ± 0.3	5.3 ± 0.2
Pulling force	Section 3.2	$5.9 \pm 0.1^{a)}$	$8.5 \pm 0.2^{a)}$	5.2 ± 0.2
AUC exp.	Section SIII A7, Supporting Information	7.41 ± 0.04	7.41 ± 0.04	5.71 ± 0.06
AUC exp.	Ref. [20]	7.59	7.59	$5.54 \pm 0.03^{b)}$

[a)] This value is calculated using Equation (1); [b)] This value is derived in conjunction with the radius obtained from Ruelle et al.[19]

Einstein–Sutherland relation in Equation (1) at the nanoscale for long observation times.

- Under the assumption of stick ($b = 6$), the hydrodynamic radius, as measured from diffusion data or from the response to drag is systematically smaller than the radius calculated directly from the partial molecular volume associated with the second virial coefficient. With this assumption, we can also verify the validity of the SES equation, which is found with 10% –15% precision.
- Using the size of the particle obtained from the partial molecular volume, the independently obtained friction coefficient and viscosity, we deduce the boundary condition on the particle with Equation (2). Averaging over all experimental and simulation data, we find small deviations from perfect stick ($\bar{b} = 5.5 \pm 0.2$). This is fully consistent with the Knudsen number for C_{60} in toluene.
- Using partial slip, all experimental and simulation data become consistent with the Stokes–Einstein–Sutherland equation (Equation (3)). Acquired potential errors are within the statistical uncertainties of 2% to 4% (cf. Table 2). This demonstrates a quantitative agreement of simulation results and carefully acquired experimental data on the validity of the SES equation, in a real system on the 1 nm length scale, and away from the infinite mass limit of the solute, which was a decades old problem.

In conclusion, our findings are instrumental to explain the reason for small or no inconsistencies of the Stokes–Einstein–Sutherland equation on the nanoscale,[17,18,20,78] despite violation of basic premise of the Mori–Zwanzig equilibrium theory.[14,43,44] As we show in our simulations and experiments, this agreement stems from extracting friction from non-equilibrium drag on the particle in simulations or the sedimentation experiments, which is in essence probing the zero frequency linear response to a net force. Notably, such extracted friction is through the Eisnstein–Sutherland equation consistent with the equilibrium diffusion coefficient of C_{60}. The very basic nature of this finding suggests that it is applicable very generally, and therefore could be systematically used to determine friction on the molecular scale. Recovering the SES equation is, however, a little more delicate—for C_{60} it requires a small partial slip on the particle surface, as suggested by a small but not negligible Knudsen number.[72,77] This finding truly benefited from the choice of the solute and the solvent, as this combination allows for the independent estimate of the hydrodynamic radius. This is more challenging in systems with flexible solutes and stronger solute-solvent interactions, and is a task that will be addressed in future work.

Supporting Information

Supporting Information is available from the Wiley Online Library or from the author.

Acknowledgements

The authors acknowledge funding by the Deutsche Forschungsgemeinschaft (DFG, German Research Foundation) through Project-ID 416229255 - SFB 1411 Design of Particulate Products (subprojects A01, C04 and D01) - and project INST 90-1123-1 FUGG. The authors gratefully acknowledge the scientific support and HPC resources provided by the Erlangen National High Performance Computing Center (NHR@FAU) of the Friedrich-Alexander-Universität Erlangen-Nürnberg (FAU). The hardware is funded by the DFG.

Open access funding enabled and organized by Projekt DEAL.

Conflict of Interest

The authors declare no conflict of interest.

Data Availability Statement

The data that support the findings of this study are openly available in Zenodo at http://doi.org/10.5281/zenodo.8281244, reference number 8281244.

Keywords

analytical ultracentrifugation, boundary condition, Green–Kubo formalism, molecular dynamics, Stokes–Einstein–Sutherland equation

Received: June 2, 2023
Revised: September 5, 2023
Published online: October 8, 2023

[1] R. Brown, in *Cambridge Library Collection - Botany and Horticulture*, Vol. *1*, Cambridge University Press, Cambridge **2015**, pp. 463–486.

[2] A. Einstein, *Ann. Phys.* **1905**, *322*, 549.
[3] W. Sutherland, *The London, Edinburgh, and Dublin Philosophical Magazine and Journal of Science* **1905**, *9*, 781.
[4] M. von Smoluchowski, *Ann. Phys.* **1906**, *326*, 756.
[5] J. Perrin, *C. R. Acad. Sci. Paris* **1908**, *146*, 967.
[6] J. Perrin, *C. R. Acad. Sci. Paris* **1908**, *147*, 475.
[7] J. Perrin, *C. R. Acad. Sci. Paris* **1908**, *147*, 530.
[8] J. Perrin, *Ann. Chim. Phys.* **1909**, *18*, 5.
[9] C. C. Miller, J. Walker, *Proc. R. Soc. London A.* **1924**, *106*, 724.
[10] P. Schuck, *Biophys. J.* **2000**, *78*, 1606.
[11] M. Sharma, S. Yashonath, *J. Phys. Chem. B* **2006**, *110*, 17207.
[12] C. M. Alexander, J. C. Dabrowiak, J. Goodisman, *J. Colloid Interface Sci.* **2013**, *396*, 53.
[13] S. Süß, C. Metzger, C. Damm, D. Segets, W. Peukert, *Powder Technol.* **2018**, *339*, 264.
[14] R. Zwanzig, *Annu. Rev. Phys. Chem.* **1965**, *16*, 67.
[15] P. Español, I. Zúñiga, *J. Chem. Phys.* **1993**, *98*, 574.
[16] Z. Miličević, *Ph.D. Thesis*, Friedrich-Alexander-Universität Erlangen-Nürnberg **2016**.
[17] R. P. Carney, J. Y. Kim, H. Qian, R. Jin, H. Mehenni, F. Stellacci, O. M. Bakr, *Nat. Commun.* **2011**, *2*, 335.
[18] H. Matsuura, S. Iwaasa, Y. Nagasaka, *J. Chem. Eng. Data* **2015**, *60*, 3621.
[19] P. Ruelle, A. Farina-Cuendet, U. W. Kesselring, *J. Am. Chem. Soc.* **1996**, *118*, 1777.
[20] J. Pearson, T. L. Nguyen, H. Cölfen, P. Mulvaney, *J. Phys. Chem. Lett.* **2018**, *9*, 6345.
[21] M. Dresselhaus, G. Dresselhaus, P. Eklund, in *Science of Fullerenes and Carbon Nanotubes* (Eds: M. Dresselhaus, G. Dresselhaus, P. Eklund), Academic Press, San Diego **1996**, pp. 60–79.
[22] K. Hedberg, L. Hedberg, D. S. Bethune, C. A. Brown, H. C. Dorn, R. D. Johnson, M. De Vries, *Science* **1991**, *254*, 410.
[23] S. Liu, Y.-J. Lu, M. M. Kappes, J. A. Ibers, *Science* **1991**, *254*, 408.
[24] P. W. Stephens, L. Mihaly, P. L. Lee, R. L. Whetten, S.-M. Huang, R. Kaner, F. Deiderich, K. Holczer, *Nature* **1991**, *351*, 632.
[25] A. Goel, J. B. Howard, J. B. V. Sande, *Carbon* **2004**, *42*, 1907.
[26] B. E. Murphy, *Ph.D. Thesis*, Trinity College Dublin **2014**.
[27] D. M. Heyes, *J. Chem. Soc., Faraday Trans.* **1994**, *90*, 3039.
[28] D. M. Heyes, M. J. Nuevo, J. J. Morales, A. C. Branka, *J. Phys.: Condens. Matter* **1998**, *10*, 10159.
[29] R. Walser, A. E. Mark, W. F. van Gunsteren, *Chem. Phys. Lett.* **1999**, *303*, 583.
[30] F. Ould-Kaddour, D. Levesque, *Phys. Rev. E* **2000**, *63*, 011205.
[31] R. Walser, B. Hess, A. E. Mark, W. F. van Gunsteren, *Chem. Phys. Lett.* **2001**, *334*, 337.
[32] F. Ould-Kaddour, D. Levesque, *J. Chem. Phys.* **2003**, *118*, 7888.
[33] J. R. Schmidt, J. L. Skinner, *J. Chem. Phys.* **2003**, *119*, 8062.
[34] J. R. Schmidt, J. L. Skinner, *J. Phys. Chem. B* **2004**, *108*, 6767.
[35] Z. Li, *Phys. Rev. E* **2009**, *80*, 061204.
[36] B. J. Alder, D. M. Gass, T. E. Wainwright, *J. Chem. Phys.* **1970**, *53*, 3813.
[37] G. G. Stokes, *Trans. Cambridge Philos. Soc.* **1851**, *9*, 8.
[38] J. G. Kirkwood, *J. Chem. Phys.* **1946**, *14*, 180.
[39] M. S. Green, *J. Chem. Phys.* **1952**, *20*, 1281.
[40] M. S. Green, *J. Chem. Phys.* **1954**, *22*, 398.
[41] R. Kubo, *J. Phys. Soc. Jpn.* **1957**, *12*, 570.
[42] R. Kubo, M. Yokota, S. Nakajima, *J. Phys. Soc. Jpn.* **1957**, *12*, 1203.
[43] R. Zwanzig, *J. Chem. Phys.* **1964**, *40*, 2527.
[44] H. Mori, *Prog. Theor. Phys.* **1965**, *33*, 423.
[45] R. Zwanzig, *Nonequilibrium Statistical Mechanics*, Oxford University Press, Oxford **2001**.
[46] B. Kowalik, J. O. Daldrop, J. Kappler, J. C. F. Schulz, A. Schlaich, R. R. Netz, *Phys. Rev. E* **2019**, *100*, 012126.
[47] L. Bocquet, J. Piasecki, J.-P. Hansen, *J. Statist. Phys.* **1994**, *76*, 505.
[48] J. O. Daldrop, B. G. Kowalik, R. R. Netz, *Phys. Rev. X* **2017**, *7*, 041065.
[49] D. van der Spoel, E. Lindahl, B. Hess, G. Groenhof, A. E. Mark, H. J. C. Berendsen, *J. Comp. Chem.* **2005**, *26*, 1701.
[50] H. Berendsen, D. van der Spoel, R. van Drunen, *Comput. Phys. Commun.* **1995**, *91*, 43.
[51] E. Lindahl, B. Hess, D. van der Spoel, *Mol. Model. Annu.* **2001**, *7*, 306.
[52] B. Hess, C. Kutzner, D. van der Spoel, E. Lindahl, *J. Chem. Theory Comput.* **2008**, *4*, 435.
[53] N. Goga, A. J. Rzepiela, A. H. de Vries, S. J. Marrink, H. J. C. Berendsen, *J. Chem. Theory Comput.* **2012**, *8*, 3637.
[54] S. Pronk, S. Páll, R. Schulz, P. Larsson, P. Bjelkmar, R. Apostolov, M. R. Shirts, J. C. Smith, P. M. Kasson, D. van der Spoel, B. Hess, E. Lindahl, *Bioinformatics* **2013**, *29*, 845.
[55] M. J. Abraham, T. Murtola, R. Schulz, S. Páll, J. C. Smith, B. Hess, E. Lindahl, *SoftwareX* **2015**, *1-2*, 19.
[56] W. L. Jorgensen, D. S. Maxwell, J. Tirado-Rives, *J. Am. Chem. Soc.* **1996**, *118*, 11225.
[57] A. Baer, P. Malgaretti, M. Kaspereit, J. Harting, A.-S. Smith, *J. Mol. Liq.* **2022**, *368*, 120636.
[58] B. Dünweg, K. Kremer, *J. Chem. Phys.* **1993**, *99*, 6983.
[59] I.-C. Yeh, G. Hummer, *J. Phys. Chem. B* **2004**, *108*, 15873.
[60] A. N. Lagar'kov, V. M. Sergeev, *Soviet Phys.-Usp.* **1978**, *21*, 566.
[61] F. Gottwald, S. Karsten, S. D. Ivanov, O. Kühn, *J. Chem. Phys.* **2015**, *142*, 244110.
[62] J. Walter, K. Löhr, E. Karabudak, W. Reis, J. Mikhael, W. Peukert, W. Wohlleben, H. Cölfen, *ACS Nano* **2014**, *8*, 8871.
[63] P. Schuck, H. Zhao, C. Brautigam, R. Ghirlando, *Basic Principles of Analytical Ultracentrifugation*, CRC Press, Boca Raton, FL **2016**.
[64] S. Uchiyama, F. Arisaka, W. Stafford, T. Laue, *Analytical Ultracentrifugation: Instrumentation, Software, and Applications*, Springer, Japan **2016**.
[65] F. J. V. Santos, C. A. Nieto de Castro, J. H. Dymond, N. K. Dalaouti, M. J. Assael, A. Nagashima, *J. Phys. Chem. Ref. Data* **2006**, *35*, 1928233.
[66] C. S. Yannoni, P. P. Bernier, D. S. Bethune, G. Meijer, J. R. Salem, *J. Am. Chem. Soc.* **1991**, *113*, 3190.
[67] R. D. Johnson, D. S. Bethune, C. S. Yannoni, *Acc. Chem. Res.* **1992**, *25*, 169.
[68] P. A. Heiney, J. E. Fischer, A. R. McGhie, W. J. Romanow, A. M. Denenstein, J. P. McCauley Jr, A. B. Smith, D. E. Cox, *Phys. Rev. Lett.* **1991**, *66*, 2911.
[69] W. Krätschmer, L. D. Lamb, K. Fostiropoulos, D. R. Huffman, *Nature* **1990**, *347*, 354.
[70] R. J. Wilson, G. Meijer, D. S. Bethune, R. D. Johnson, D. D. Chambliss, M. S. de Vries, H. E. Hunziker, H. R. Wendt, *Nature* **1990**, *348*, 621.
[71] K. Koga, B. Widom, *J. Chem. Phys.* **2013**, *138*, 114504.
[72] Z. Li, H. Wang, *Phys. Rev. E* **2003**, *68*, 061206.
[73] A. Tuteja, M. E. Mackay, S. Narayanan, S. Asokan, M. S. Wong, *Nano Lett.* **2007**, *7*, 1276.
[74] L. G. Longsworth, *J. Am. Chem. Soc.* **1952**, *74*, 4155.
[75] P. Y. Cheng, H. K. Schachman, *J. Polym. Sci.* **1955**, *16*, 19.
[76] M. I. M. Feitosa, O. N. Mesquita, *Phys. Rev. A* **1991**, *44*, 6677.
[77] E. Cunningham, J. Larmor, *Proc. R. Soc. London A.* **1910**, *83*, 357.
[78] R. Jin, H. Qian, Z. Wu, Y. Zhu, M. Zhu, A. Mohanty, N. Garg, *J. Phys. Chem. Lett.* **2010**, *1*, 2903.